A framework recommendation for updating running safety design criteria of non-ballasted railway bridges using statistical investigations

R Allahvirdizadeh, A Andersson and R Karoumi

Division of Structural Engineering & Bridges, KTH Royal Institute of Technology, Stockholm, Sweden

E-mail: rezaal@kth.se

Abstract. As far as the authors are aware, the threshold for vertical acceleration of the bridge deck was chosen based on the assumption that the induced dynamic loads would overcome gravity at higher accelerations, resulting in loss of contact between wheels and rail; however, the previous studies do not support this hypothesis. Considering these inconsistencies, a better understanding of the simplified design criteria is essential before conducting further studies such as the calibration of partial safety factors. Therefore, this study considers a set of representative design scenarios to statistically compare wheel-rail contact loss with other criteria that can be derived from moving load models, such as vertical accelerations and bridge deck deflections. Based on the analyzes performed, deflection seems to be a better criterion than acceleration to control the running safety limit-state; although the results presented do not necessarily show a very strong correlation between these two criteria. Therefore, the k-means clustering approach is used together with 5% lower quantiles of the collected data to propose potential new thresholds. It should be noted that due to the limited number of analyzes, the approach presented in this study can be considered as a possible framework for further updates of the current design method rather than drawing general conclusions.

1. Introduction

The safe passage of trains over bridges, i.e. preventing train derailments, requires that contact between coach wheels and rails be assured. This is the concern of *running safety* limit-state in the design procedure of railway bridges with respect to dynamic loading scenarios. Traditionally, this is controlled by limiting the vertical acceleration of the bridge deck that has its roots on ballast destabilization phenomenon of ballasted tracks. The latter can be traced back to a series of shaking table tests conducted by Zacher and Baeßler [1], in which they recorded the lateral displacement of the sleepers as an indicator of ballast instability as a function of vertical acceleration of the specimens. They found that at accelerations greater than 7.0 $\mathrm{m/s^2}$, the lateral displacement increases significantly. This threshold is the one specified in the regulations for the running safety limit state of ballasted tracks [2]. In addition, a safety factor of 2.0 is considered in this procedure by the design standards [3]; however, to the authors' knowledge, it is not calibrated by performing partial safety calibration approaches introduced in the field of structural reliability. In [4], this aspect is pointed out by highlighting the inconsistency between the safety indices determined by the first-order reliability method (FORM) for bridges with different span lengths. Moreover, simulation-based probabilistic evaluations were performed in [5], which showed that the loss of wheel-rail contact in ballasted tracks occurs only after violation of the acceleration-based criteria.

An identical approach is applied from ballasted tracks to non-ballasted tracks, assuming that wheel-rail contact is lost at accelerations above 10.0 m/s^2. This assumption is based on the assumption that the dynamic forces counteract the inertial forces (especially the car weight) at accelerations greater than 1.0g (unloading phenomenon). Then, a partial safety factor similar to that used for ballasted tracks is used in the design regulations [3]. The applicability of this partial safety factor is investigated by performing a series of preliminary reliability evaluations for simply supported single-span bridges with short to medium spans using the tail-modelling approximation, establishing the possibility of their improvement (most likely reduction) [6]. It is worth mentioning here that the Japanese standard controls the running safety limit-state by deflection-based criteria that depend on both the bridge span and the operating speed of the passing train [7].

Such implicit consideration of running safety can be promoted by its applicability to computational models that neglect train-track-bridge interaction (TTBI). These models replace the structure of passing trains with moving loads, which greatly increases the computational efficiency of the models, although accuracy suffers somewhat and some aspects of the problem (mainly those related to the train itself) can no longer be studied. For example, it has been shown that the models with moving loads underestimate the damping of the system, leading to an overestimation of the responses, especially under resonant conditions [8, 9]. However, such differences become less critical for cases with a low ratio of coach to bridge mass [10], so that consideration of TTBI becomes more important for bridges with shorter spans in general (i.e., bridges with spans less than 30 m) [11]. In view of this, the limit-state of running safety cannot be explicitly investigated with moving load models.

When using models with TTBI, the unloading ratio and derailment factor can be calculated at each step of the analysis, which are believed to better represent the wheel-rail contact loss phenomenon. These ratios can be formulated as Eq.(1) [12] and Eq.(2) [13]. The latter describes the situation where the vertical load cannot prevent the lateral load from forcing the wheel to climb above the rail [14].

$$\frac{\Delta p}{p_{\mathrm{st}}} = \frac{p_{\mathrm{st}} - \min\left[p_{\mathrm{dyn}}\right]}{p_{\mathrm{st}}} \tag{1}$$

$$\frac{p_{\mathrm{lat}}}{p_{\mathrm{dyn}}} = \frac{\tan[\alpha] - \mu}{1 + \mu\tan[\alpha]} \tag{2}$$

where p_{st}, p_{dyn} and p_{lat} are the static vertical load, dynamic vertical load and dynamic lateral load, respectively. Also, α is the contact angle (i.e., the angle between the wheel-rail friction force and the horizontal axis) and μ is the friction coefficient. From a theoretical point of view, it is clear that the wheel-rail contact is lost when the unloading ratio is 1.0, while other conservative values such as 0.6, 0.8 or 0.9 can be found in various references as design thresholds [12, 7, 15, **?**]. On the other hand, the derailment factor is considered to occur at values greater than 0.8 when the duration of the exeedence is greater than a prescribed value, e.g., 50 ms according to the Japanese National Railway (JNR) standard [7]. The other approach to consider the duration of contact loss is to filter the forces through a low-pass filter (often with a cutoff frequency of 20 Hz). At this point, it should be emphasized that the unloading ratio can be evaluated with both 2D and 3D models, while the evaluation of the derailment factor requires the construction of 3D models, which require a higher computational budget. Therefore, in this study, the unloading ratio is used to investigate the running safety phenomenon of non-ballasted railway bridges. Since the main objective of the article is to propose a framework for revising the codified thresholds, the approach proposed in [17] is followed here by assuming no safety margin for the unloading ratio.

The rest of the article is divided into the description of the computational modeling approach used, a brief explanation of the methodology employed, the presentation of the results obtained, and the conclusion of the article with its main highlights.

2. Modelling strategy and parameters

The computational model used to study the running safety problem for non-ballasted tracks is shown schematically in Figure 1. This 2D finite element model consists of the bridge structure, the slab track, the rail (with possible irregularities), the passing train, and their interactions (i.e., slab subgrade, rail pad, and wheel-rail contact). At this point, it should be emphasized that only single-span, simply-supported reinforced concrete railway bridges with spans in the range of $L = [10.0 - 50.0]$ m are considered in this study. In addition, the effects of soil-structure interaction are neglected. The bridge deck, slab tracks, and rails are modeled using 2D Euler-Bernoulli beams. In addition, the slab subgrade is modelled by distributed springs and dashpots (k_{ss} and c_{ss}), while the interaction between the rails and slab track (rail pads) are modelled by lumped springs and dashpots (k_{rs} and c_{rs}) spaced at constant $s = 0.6$ m intervals. These properties are assigned based on the recommendations of [18].

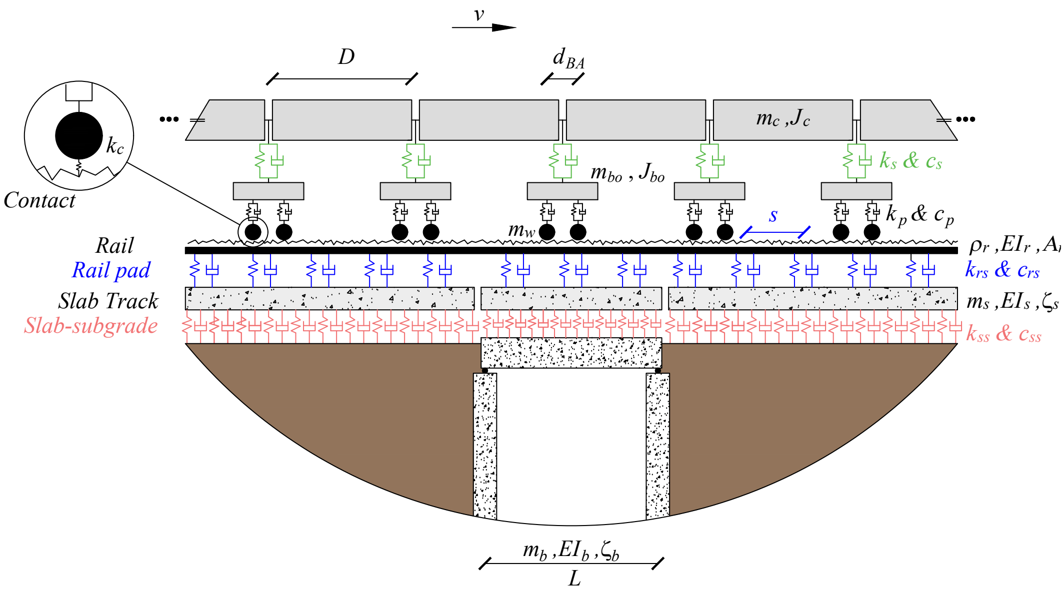

Figure 1: Schematic representation of the computational model.

The cross-sectional properties of the bridge deck can vary considerably from case to case, especially with different bridge spans and cross-section types, while the properties of slab tracks and rails are almost standardized. The nominal values of bridge moment of inertia and mass per length are determined by optimizing the cross-section dimensions with the aim of satisfying current design codes. It should be noted that the maximum permissible operating speed of trains during such optimizations is limited to 400 km/h. In addition, three general types of railway bridge cross sections are considered, namely beam, slabs and box-girder. The optimized values as a function of bridge span are shown in Figure 2. Regarding the material properties of the bridges, a nominal value of the elastic modulus of $E_{\mathrm{b}} = 29.7$ GPa is considered, based on the recommendations of [19]. Moreover, the Rayleigh method is used to model the damping of the system. In this context, the nominal value of the damping ratio for the bridge is assumed as proposed in [8], which reads as Eq. (3).

$$\xi_b = \max\left[1.5 + 0.07(20 - L), 1.5\right] \tag{3}$$

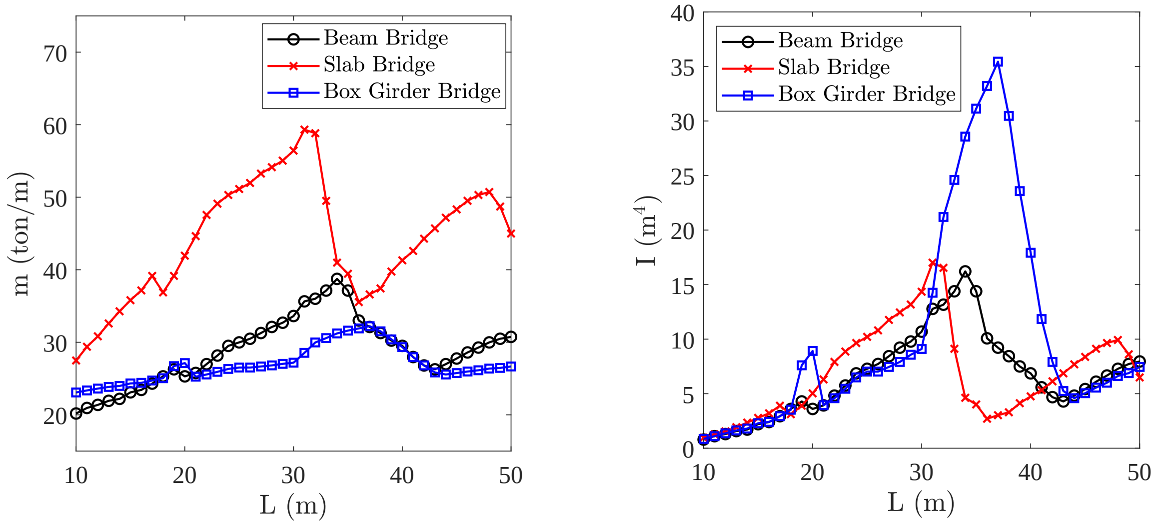

(a) Optimized mass per length

(b) Optimized moment of inertia

Figure 2: Optimized mass and moment of inertia for the considered bridges.

The UIC60 rail is considered to assign the nominal values of the rails based on the values given in [18]. Since the constructed FE models are 2D models, the cross-sectional area and moment of inertia of the rails are multiplied by 2.0 to account for the contributions of both rails. In addition, slab tracks are assumed to be rectangular blocks whose dimensions are also taken from [18].

Possible imperfections of the rail geometry, called rail irregularities, are implemented in the computational model by random realizations of the deviation from the ideal geometry. This is achieved by computing the inverse Fourier transform of random process realizations described by the power spectral density (PSD) with random phase. In this study, the German PSD is used, which reads as Eq.(4):

$$S(\Omega) = \frac{A\Omega_c^2}{(\Omega_c^2 + \Omega^2)(\Omega_r^2 + \Omega^2)} \tag{4}$$

where $\Omega_c = 0.0206$ rad/m, $\Omega_c = 0.8246$ rad/m, and $A = 0.645 \times 10^{-7}$ rad.m [20]. It should be mentioned that the latter applies to good quality tracks, which seems to be the case for high-speed lines; however, for poor quality tracks, the amplification factor changes to $A = 4.032 \times 10^{-7}$. Thus, the realization of rail irregularities can be achieved with the help of:

$$RI(x) = \sqrt{2} \sum_{n=0}^{N-1} \sqrt{\frac{1}{\pi} S(\Omega_n) \Delta\Omega} \cos\left(\Omega_n x + \varphi_n\right) \tag{5}$$

where N is the number of discrete frequencies considered, $\Omega_n = n\Omega_u/N$, Ω_u is the largest frequency considered, and φ_n is a random number in the range $[0, 2\pi]$ [21]. It should be mentioned here that wavelengths in the range 1-150 m are considered in this study. The previous studies have emphasized the importance of rail irregularities in the evaluation of running safety. Therefore, the investigations were first conducted assuming good track quality, with a very low probability that the unloading ratio exceeds the prescribed thresholds. Then, the amplification factor is changed for the poor track quality at the second stage to find the situation where wheel-rail contact loss occurs.

The passing trains are modelled as a combination of individual cars with 10 degrees of freedom (DOF) and common bogies. The wheels of these cars are lumped masses connected via springs and dashpots of the primary suspension system (k_{p} and c_{p}) to the bogie, which in turn is connected via springs and dashpots of the secondary suspension system (k_{s} and c_{s}) to the main body. It should be mentioned that the bogie and the main body are modelled as rigid bars with mass and moment of inertia. The authors did not have access to the exact (reliable) values for the contributing train properties. Therefore, it was decided to perform the simulations for a single train configuration, i.e. ICE 2 [22]. It should be emphasized here that such a selection does not allow general conclusions to be drawn, as it does not necessarily lead to an upper bound on the possible dynamic excitations. An alternative approach was to fit the HSLM loading models from [2] with reasonable train properties; which is neglected here.

The contact between wheels and rails is modelled using linearized Hertz contact. This approach allows the computational model to account for wheel-rail contact losses by describing the contact conditions (CC) as an Eq. (6):

$$CC = \begin{cases} \frac{3}{2} Q_{\mathrm{C}}^{1/3} C_{\mathrm{H}}^{2/3} \Delta u_{\mathrm{w-r}}, & \Delta u_{\mathrm{w-r}} > 0 \\ 0, & \Delta u_{\mathrm{w-r}} \leq 0 \end{cases} \tag{6}$$

where Q_{C} is the contact force, $C_{\mathrm{H}} = 2E_{\mathrm{r}}(R_{\mathrm{w}}R_{\mathrm{r}})^{1/4}/3(1-\nu_{\mathrm{r}}^2)$, E_{r} is the elastic modulus of the rail and wheel, R_{w} is the radius of the wheel, R_{r} is the radius of the rail, and ν_{r} is its Poisson's ratio. Also, $\Delta u_{\mathrm{w-r}} = u_{\mathrm{w}} - u_{\mathrm{r}} - r_{\mathrm{w}}$ is the relative deflection of the wheel (u_{w}), the rail (u_{r}) and the rail irregularity (r_{w}). As you can see, the contact condition depends on the contact force, which has to be estimated in an iterative way. In this context, first the contact force of the previous iteration is considered, then the system of equations is solved and the new contact force is calculated. Considering the described modelling aspects, the assigned properties are summarized in Table 1.

Thus, the equations of motion for the considered system reads as Eq.(7).

$$\begin{bmatrix} \mathbf{M}_{\mathrm{V}} & 0 & 0 \\ 0 & \mathbf{M}_{\mathrm{T}} & 0 \\ 0 & 0 & \mathbf{M}_{\mathrm{B}} \end{bmatrix} \begin{Bmatrix} \ddot{\mathbf{x}}_{\mathrm{V}} \\ \ddot{\mathbf{x}}_{\mathrm{T}} \\ \ddot{\mathbf{x}}_{\mathrm{B}} \end{Bmatrix} + \begin{bmatrix} \mathbf{C}_{\mathrm{V}} & 0 & 0 \\ 0 & \mathbf{C}_{\mathrm{T}} & \mathbf{C}_{\mathrm{T,B}} \\ 0 & \mathbf{C}_{\mathrm{B,T}} & \mathbf{C}_{\mathrm{B}} \end{bmatrix} \begin{Bmatrix} \dot{\mathbf{x}}_{\mathrm{V}} \\ \dot{\mathbf{x}}_{\mathrm{T}} \\ \dot{\mathbf{x}}_{\mathrm{B}} \end{Bmatrix} + \begin{bmatrix} \mathbf{K}_{\mathrm{V}} & \mathbf{K}_{\mathrm{V,T}} & 0 \\ \mathbf{K}_{\mathrm{T,V}} & \mathbf{K}_{\mathrm{T}} & \mathbf{K}_{\mathrm{T,B}} \\ 0 & \mathbf{K}_{\mathrm{B,T}} & \mathbf{K}_{\mathrm{B}} \end{bmatrix} \begin{Bmatrix} \mathbf{x}_{\mathrm{V}} \\ \mathbf{x}_{\mathrm{T}} \\ \mathbf{x}_{\mathrm{B}} \end{Bmatrix} = \begin{Bmatrix} \mathbf{F}_{\mathrm{V}} \\ \mathbf{F}_{\mathrm{T}} \\ \mathbf{F}_{\mathrm{B}} \end{Bmatrix} \tag{7}$$

where $\mathbf{M}$, $\mathbf{C}$, $\mathbf{K}$, and $\mathbf{F}$ represent mass, damping, stiffness, and load matrices, respectively. The indices of V, T and B correspond to the vehicle (passing train), track and bridge, respectively. Thus, the matrices with two indices represent the interaction between the corresponding subsystems. The matrices coupling the train with the track are time dependent, i.e. they have to be updated depending on the train location. Then, the system of equations is solved using Newmark's average acceleration method. It should be mentioned here that the discussed model was implemented in MATLAB by [20, 23]; therefore, the interested reader is referred to these references for further details.

3. Methodology and Results

As mentioned earlier, the first phase of the analyzes assumes good track quality. An example of maximum vertical acceleration as a function of train operating speed is shown in Figure 3a. In this case, no loss of contact was observed for train speeds in the range of [100-400] km/h in any of the situations considered. Therefore, no judgment could be made about possible relationships between contact loss and other measures. Track quality is then assumed to be poor, with an

Table 1: Assigned properties for the contributing variables.

Component	Variable	Value
Bridge	m_{b} - Mass per length [kg/m]	Figure 2a
	I_{b} - Moment of inertia [m^4]	Figure 2b
	E_{b} - Modulus of elasticity [GPa]	29.7
	ξ_{b} - Damping ratio [%]	Eq.(3)
Train †	m_{c} - Car-body mass [kg]	60768/33930
	J_{c} - Car-body mass moment of inertia [kg.m^2]	$1344/2115 \times 10^3$
	D - Car-body length [m]	13.0/20.25
	m_{bo} - Bogie mass [kg]	5600/2373
	J_{bo} - Bogie mass moment of inertia [kg.m^2]	21840/1832
	d_{BA} - Bogie length [m]	3.0/2.5
	k_{p} - Primary suspension stiffness [kN/m]	4800/1600
	c_{p} - Primary suspension damping [kNs/m]	108/20
	k_{s} - Secondary suspension stiffness [kN/m]	1760/300
	c_{s} - Secondary suspension damping [kNs/m]	152/6.0
	m_{w} - Wheel mass [kg]	2003/1728
Rail	E_{r} - Modulus of elasticity [GPa]	210
	A_{r} - Cross section Area [m^2]	$2 \times 7.69 \times 10^{-3}$
	I_{r} - Moment of inertia [m^4]	$2 \times 3.055 \times 10^{-5}$
	m_{r} - Mass per length [kg/m]	60.3
Slab track	b_{s} - Slab width [m]	2.5
	t_{s} - Slab thickness [m]	0.3
	ρ_{s} - Slab mass density [kg/m^3]	2500
Rail pad	k_{rs} - Lumped spring stiffness [MN/m]	2×22.5
	c_{rs} - Lumped dashpot damping [kNs/m]	2×5.47
Slab subgrade	k_{ss} - Spring stiffness [MN/m^3]	100
	ξ_{ss} - Damping ratio [%]	2.0

† The first values correspond to the locomotive car and the second one corresponds to the passenger cars.

example of the observed responses for the bridges with conditions similar to Figure 3a shown in Figure 3b. In this case, no contact forces were observed for the low-pass filtered responses at some situations, which can be considered an indicator of loss of wheel-rail contact, although this seems to be a very conservative criterion.

Subsequently, for computational cost reasons, the critical speeds of the individual bridges were calculated according to Eq. (8) and then the maximum experienced responses were evaluated.

$$v_{\mathrm{cr}} = \frac{D f_j}{k} \quad j = 1, 2, 3, ... \quad k = 1, 2, 3, ..., 1/2, 1/3, ... \tag{8}$$

where D is the length of the car-body, f_j is the frequency of the j-th mode of vibration, and k is an integer. It should be mentioned here that only the critical speed corresponding to the fundamental mode of vibration is considered.

Scatter plots of maximum vertical acceleration and deflection as a function of bridge span are shown in Figure 4. The significant variation in the maximum vertical acceleration does not allow conclusions to be drawn about its applicability to the running safety criteria; however, a clearer trend can be seen in the deflections. Therefore, further investigation will be devoted only to deflections and not to acceleration. However, as mentioned above, the results presented should not be considered as general conclusions, since only one train configuration was considered in the analyzes.

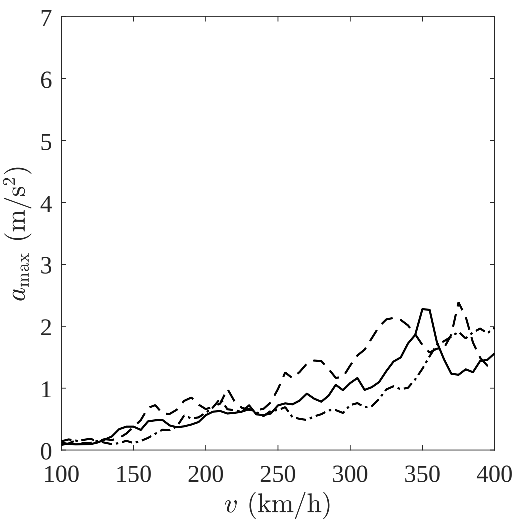

(a) Good track quality

(b) Poor track quality

Figure 3: Example of maximum vertical acceleration of bridge deck as a function of operating train speed.

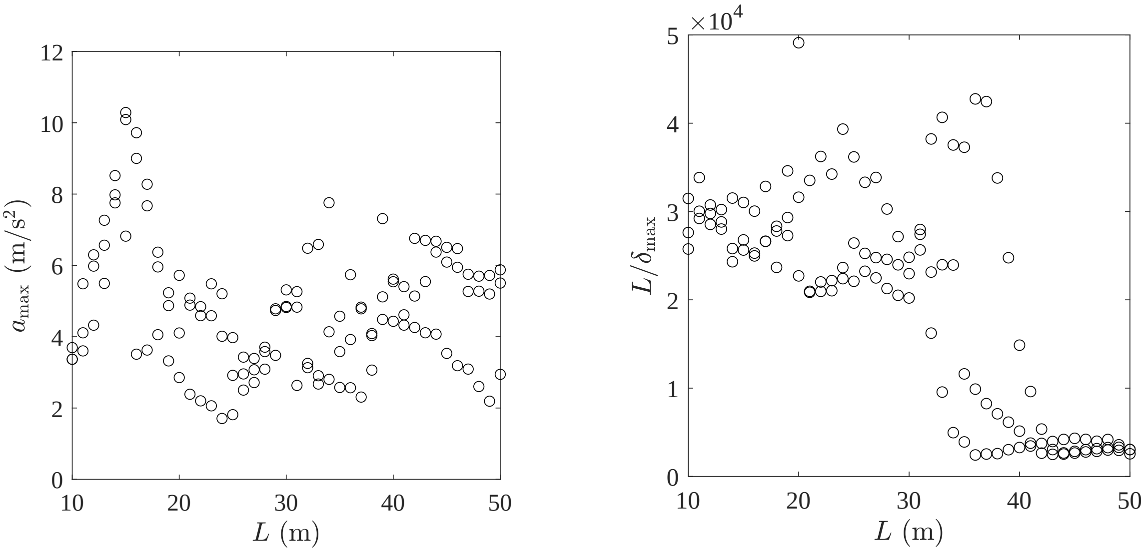

(a) Maximum vertical acceleration

(b) Maximum deflection

Figure 4: Scatter of the maximum vertical acceleration and deflection as a function of bridge span length.

First, the collected data for the maximum deflection of the bridges were clustered using the k-means algorithm; which each cluster are shown in Figure 5a. It is worth noting that the k-means algorithm is a distance-based method that partitions the data points based on their distance from each other. In addition, it should be noted that for better illustration, a natural logarithmic transformation is applied to the data points in Figure 5a. To check the consistency of the clustering, the silhouette values were computed. The latter basically compare the similarity of each point with the other points within that cluster and reads as Eq. (9).

$$s_i = \frac{x_i - x_i'}{\max\left(x_i, x_i'\right)} \tag{9}$$

where x_i is the average distance of the ith point to points in the identical cluster, x_i' is the minimum average distance of the ith point to points in other clusters. Thus, the silhouette value varies in the range of [-1,1]. The higher the value, the better the points within an identical cluster match together and the better they are separated from points in other clusters. Considering this, the clusters shown in Figure 5a seem to be acceptable for the goal of the current study.

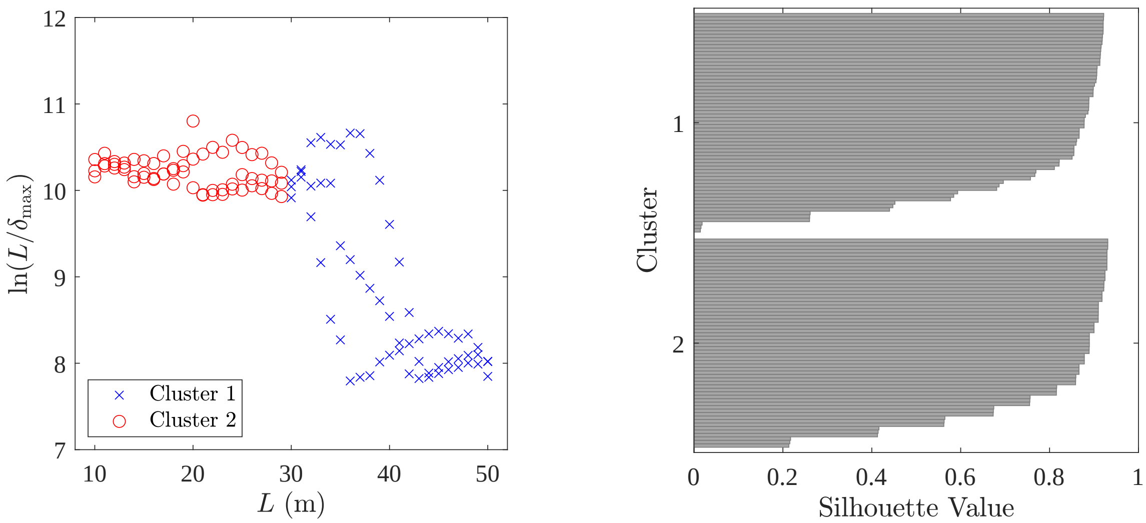

(a) Clusters of maximum deflection

(b) Silhouette plot of the clusters

Figure 5: Clustering the collected data corresponding to the maximum deflection of the bridges.

Then, the 5% quantiles of the points within each cluster are calculated to be considered as possible values for the running safety criteria; the values obtained are as Eq. (10).

$$\gamma = \ln\left(\frac{L}{\delta_{\max}}\right) = \begin{cases} 9.95 & L \leq 30\text{m} \\ 7.80 & L > 30\text{m} \end{cases} \tag{10}$$

4. Conclusions

In this study, a statistical approach is taken to propose a possible framework that can be used to update the current running safety design criteria of non-ballasted railway bridges. These criteria are based on the maximum vertical acceleration of the bridge deck at the moment. However, the results presented showed a large scatter in the observed accelerations corresponding to wheel-rail contact loss situations. Therefore, the maximum vertical acceleration does not seem to be a reliable design criterion for the goal of running safety. A smaller scatter was observed for the maximum deflection of the bridge, but this does not necessarily mean that there is a strong correlation between wheel-rail contact loss and maximum deflection. Nevertheless, the collected data points were clustered and the 5% lower quantile values were suggested as possible values to be used as design criteria for running safety. It should be noted that the values presented in this study were based on limited design scenarios and only one type of train configuration. Therefore, general conclusions for further applications should not be drawn based on these values, but the proposed method can be considered as a possible framework for updating the current criteria.

Acknowledgments

This project has received funding from the Shift2Rail Joint Undertaking under the European Union's Horizon 2020 research and innovation programme under grant agreement No. 101012456.

References

[1] Zacher M and Baeßler M 2008 *Dynamic behaviour of ballast on railway bridges*, in: Dynamics of High–Speed Railway Bridges (CRC Press).

[2] CEN 2003 *EN 1991-2, Eurocode 1: Actions on structures - part 2: Traffic loads on bridges* (European Committee for Standardization).

[3] CEN 2005 *EN 1990/A1, Basis of structural design annese A2* (European Committee for Standardization).

[4] Allahvirdizadeh R, Andersson A and Karoumi M 2020 Reliability assessment of the dynamic behavior of high-speed railway bridges using first order reliability method, *Eurodyn 2020, 11th International Conference on Structural Dynamics* (Athens, Greece).

[5] Rocha J M, Henriques A A and Calcada R 2016 Probabilistic assessment of the train running safety on a short-span high-speed railway bridge, *Structure and Infrastructure Engineering* **12**(1), 78-92.

[6] Allahvirdizadeh R, Andersson A and Karoumi M 2020 Estimating running safety factor of ballastless railway bridges using tail modelling, *IPW 2022, 19th International Probabilistic Workshop* (Stellenbosch, South Africa).

[7] RTRI 2007 *Design standards for railway structures and commentary (displacement limits)* (Railway Technical Research Institute, Railway Bureau of the Ministry of Land, Infrastructure and Transport Government of Japan).

[8] ERRI D214 1999 *RP 4 Rail bridges for speeds > 200 km/h - train-bridge interaction* (European Rail Research Institute).

[9] Yau J, Martinez-Rodrigo M D and Domenech A 2019 An equaivalent additional damping approach to assess vehicle-bridge interaction for train induced vibration of short-span railwa bridges, *Engineering Structures* **188** 469–479.

[10] Yang Y and Yau J 1998 Vehicle-bridge interactions and applications to high-speed rail bridges, *Proceedings of the National Science Council* **22**.

[11] Arvidsson T and Karoumi R 2014 Train-bridge interaction - a review and discussion of key model parameters, *International Journal of Rail Transportation* **2**(3), 147-186.

[12] CEN 2016 *EN 14363, Railway applications - testing and simulation for the acceptance of running characteristics of railway vehicles - running behaviour and stationary tests* (European Committee for Standardization).

[13] Nadal J 1908 Locomotives à vapeur, *Encyclopédie scientifique* (Bibliothèque de mécanique appliqueée et génie. O. Doin, Paris).

[14] Arvidsson T, Andersson A and Karoumi R 2019 Train running safety on non-ballasted bridges, *International Journal of Rail Transportation* **7**(1), 1-22.

[15] EN 14067-6 2010 *Railway applications – aerodynamics – Part 6: requirements and test procedures for cross wind assessment* (European Committee for Standardization).

[16] TB 10002-2017 2017 *Code for Design on Railway Bridge and Culvert* (Beijing: People's Republic of China National Railway Administration, CNRA-PRC).

[17] Rocha J M, Henriques A A, Calcada R and Rönnquist A 2015 Efficient methodology for the probabilistic safety assessment of high-speed railway bridges, *Engineering Structures* **101**, 138-149.

[18] Arvidsson T, Andersson A and Karoumi R 2019 Train running safety on non-ballasted bridges, *International Journal of Rail Transportation*, **7**(1), 1-22.

[19] Wisniewski D F 2007 *Safety formats for the assessment of concrete bridges: with special focus on precast concrete*, PhD Dissertation, University of Minho.

[20] Cantero D, Arvidsson T, OBrigen E and Karoumi R 2016 Train-track-bridge modelling and review parameters, *Structures and Infrastructure Engineering*, **12**(9), 1051-1064.

[21] Claus H and Schiehlen W 1998 Modeling and Simulation of Railway Bogie Structural Vibrations, *Vehicle System Dynamics Supplement*, **28**, 538-552.

[22] Domenech A, Museros P and Martinez-Rodrigo L 2014 Influence of the vehicle-structure interaction in the design of high-speed railway bridges, *Proceedings of 2nd International Conference on Railway Technology: Research, Development and Maintenance* (Stirlingshire, Scotland).

[23] Arvidsson T 2018 *Train–track–bridge interaction for the analysis of railway bridges and train running safety* PhD Dissertation, KTH Royal Institute of Technology.